ELSEVIER

Biophysical Chemistry 67 (1997) 187–198

Biophysical Chemistry

Strong and weak binding of water to proteins studied by NMR triple-quantum filtered relaxation spectroscopy of ^{17}O-water

Allan M. Torres, Stuart M. Grieve, Bogdan E. Chapman, Philip W. Kuchel *

Department of Biochemistry, the University of Sydney, Sydney, N.S.W. 2006, Australia

Received 13 November 1996; revised 13 March 1997; accepted 14 March 1997

Abstract

The triple-quantum filtered (TQF) spin-echo signal of ^{17}O-water, in the presence of proteins, was analysed to yield estimates of the number of weakly, and strongly bound water molecules. The analysis used a constrained direct iterative regression procedure with a three-state model of fast-exchange. Thus, the population size of free, weakly, and strongly bound water were determined simultaneously. The two fractions of the bound water were estimated by using correlation time(s) estimated in other studies. Bovine serum albumin (BSA), basic pancreatic trypsin inhibitor (BPTI), lysozyme and oxyhaemoglobin were studied. Of the four proteins, BSA contained the largest number of strongly and weakly bound water molecules, there being ~ 30 of the former and ~ 3000 of the latter under conditions of high protein concentration. The correlation time of the proteins increases with their concentration in solution, and when this was taken into account for BSA the estimated number of strongly bound water molecules did not change significantly. This NMR technique, and data analysis, will probably also be useful in studies of water binding and mobility in various systems including hydrogels, protein networks, membranes, cells and tissues. © 1997 Elsevier Science B.V.

Keywords: Bound water; Hydration; NMR; ^{17}O-water; Protein–water interaction; Triple-quantum filtered spectra

1. Introduction

Water is the major component of living systems where it plays an important role in a myriad of processes both inside and outside cells. Thus, numerous studies have been performed over many years to determine the properties and activities of water, especially its interactions with various biomolecules [1–6]. One way of 'seeing' that the properties of water inside cells is different from outside is via the NMR 'split peak phenomenon' [7,8]. This effect is apparent when suspensions of erythrocytes [7,8] or other cells [9] are supplemented with certain phosphorus compounds such as hypophosphite ($H_2{}^{31}PO_2^-$), fluorinated compounds such as 3-^{19}F-3-deoxy-D-glucose [10], and compounds such as ^{13}C-formate [11]; separate resonances (peaks) from the nuclear populations inside and outside the cells are seen in the respective NMR spectra. The fact that the NMR-receptive nuclei resonate at different frequencies, inside and outside the cells, has been shown to be primarily a solvent effect, rather than an effect of different magnetic susceptibilities inside and outside the cells, although this may pertain as well. The split peaks are a manifestation of the altered average

* Corresponding author. Tel.: (+61-2)93513709; fax: (+61-2)93514726.

PII S0301-4622(97)00039-2

extent of hydrogen-bonding between solutes and water inside the cells, brought about by the relatively high protein concentration inside [12]. The motivation of the present work was the quest for an alternative means for probing the interactions of solutes and water in cellular systems, as part of a more general physical-chemical characterisation of cells (e.g., [13]).

The simplest model of water in biological systems has three different physical states, namely free water, water weakly bound to biomolecules (or vicinal water), and water that is strongly bound [1]. The free water is regarded as being unperturbed, since its properties are similar to those of pure water; on the other hand, strongly bound water is envisaged as being tightly bound to biomolecules via hydrogen bonds and thus has a long correlation time. It is supposed that weakly bound water is primarily associated with biomolecular surfaces [4]. Such water molecules are known to be numerous but their residence time at the surface sites is short, with correlation times that lie between those of pure water and strongly bound water.

In previous work [6], we studied the binding of ^{17}O-water in protein solutions by analysing the relaxation of transverse and longitudinal nuclear-magnetic coherences that were subjected to a triple-quantum filter (TQF). These analyses proved to be useful for estimating the population size of strongly bound water, since only highly immobilized water produces a TQF signal [5]. In the model adopted for the data analysis it was assumed that there are only two states of water (free and tightly bound) which undergo fast interchange. Although this two-state model is sufficient to account for the above properties of strongly bound water, the analysis was inadequate for characterising the free water. This shortcoming was manifested in the fact that the longitudinal relaxation rate-constant of free water, calculated from the data, was larger than that actually measured in a simple inversion recovery experiment on pure water. We attributed this discrepancy to the relaxation contributions from vicinal or weakly bound water; in other words the two-state model is fundamentally inconsistent with the data. Thus, in the present work we extended the model, confirmed its utility in studies of water binding to BSA, and then applied it to three other proteins.

A data regression procedure for analysing triple-quantum filtered (TQF) *spin-echo* signals was implemented and its utility for estimating the values of relaxation parameters was evaluated. Thus, analysis of the relaxation in the transverse plane of the TQF signal from ^{17}O-water was applied to solutions of bovine serum albumin (BSA), basic pancreatic trypsin inhibitor (BPTI), lysozyme and oxyhaemoglobin.

2. Theory

2.1. Basic principles

The NMR relaxation behaviour of quadrupolar nuclei, such as those in ^{17}O-water, is best described by using the irreducible tensor operator formalism; comprehensive descriptions of the use of these operators are found elsewhere [14–16] so they are not dealt with in detail here. It is assumed in the following discussion that all relevant matrices are expressed in this operator basis-set and that coherence-relaxation is due to quadrupolar coupling interactions.

For a quadrupolar spin system with several states, undergoing fast chemical exchange, the relaxation rate constant for a given coherence order, n, is a weighted average relaxation rate constant of the different states, i, [17]. This is formally expressed by,

$$\boldsymbol{R}^{(n)}_{\text{system}} = \sum_i p_i \boldsymbol{R}^{(n)}_i \qquad (1)$$

where $\boldsymbol{R}$ is the Redfield relaxation matrix which contains terms involving quadrupolar coupling constants and spectral density functions, J, that are expressed in terms of the correlation time τ_c; $\boldsymbol{R}^{(n)}_{\text{system}}$ is the resulting relaxation matrix; $\boldsymbol{R}^{(n)}_i$ is the corresponding relaxation matrix for state i, in the absence of chemical exchange. For spin-$\frac{5}{2}$ nuclei, the relaxation matrices are square with 5×5 dimensions. In the present NMR study, in which only odd-rank tensor-operators are important, the dimensions of this matrix can be reduced to 3×3 [15]. The relaxation matrix $\boldsymbol{R}^{(n)}_{\text{system}}$ has all the information that determines the quadrupolar relaxation behaviour of the system; for example, parameters such as longitudinal and transverse relaxation rate constants, as well as

those that determine the decay of triple-quantum signals, can be extracted from the values of the elements of this hybrid relaxation-rate-constant matrix. Basically, this analysis is performed by first diagonalizing the relaxation-rate-constant matrix $\boldsymbol{R}^{(n)}_{\text{system}}$ as represented by the equation:

$$\boldsymbol{R}^{(n)}_{\text{system}} = \boldsymbol{V}^{(n)-1}\boldsymbol{R}^{(n)}_{\text{diag}}\boldsymbol{V}^{(n)} \tag{2}$$

where $\boldsymbol{V}^{(n)}$ is the eigenvector matrix and $\boldsymbol{R}^{(n)}_{\text{diag}}$ is the eigenvalue matrix with diagonal elements $\boldsymbol{R}^{(n)}_{q}$. The coherence decay (relaxation) function matrix is:

$$f^{(n)}(t) = \boldsymbol{V}^{(n)-1}\exp\left(-\boldsymbol{R}^{(n)}_{\text{diag}}t\right)\boldsymbol{V}^{(n)} \tag{3}$$

It has elements which can be written in the form:

$$f^{(n)}_{p'p'}(t) = \sum_{q=1}^{5} \boldsymbol{V}^{(n)}_{qp'}\boldsymbol{V}^{(n)}_{qp'}\exp\left(-\boldsymbol{R}^{(n)}_{q}t\right) \tag{4}$$

where the subscripts refer to the corresponding row and column addresses of each element [15]. The decay function is of practical value since it describes the relaxation behaviour of the different coherences. For example, the NMR signal decays with the rate constant $f^{(0)}_{11}(t)$ for the longitudinal signal (inversion recovery), $f^{(1)}_{11}(t)$ for the transverse signal (spin-echo), $f^{(1)}_{31}(t)$ for the transverse TQF signal, and $f^{(0)}_{31}(t)$ for the longitudinal TQF signal.

Knowledge of the relaxation behaviour of ^{17}O-water coherences via various NMR relaxation experiments, therefore, provides information on the fraction p_i and/or correlation times τ_c of the different states of water in the solution. Such information can be explicitly obtained, for example, by iterative statistical regression of the theoretical decay function $f^{(1)}_{31}(t)$ onto the observed decay profile. TQF experiments are particularly useful for studying protein hydration since these signals are created only by strongly bound ^{17}O-water spins whose correlation times are expected to be greater than $\sim$ 1 ns.

In the water-of-hydration model adopted in our previous work [6], it was assumed that there were only two states of water which are in fast exchange, viz., water strongly bound to the protein and water free in solution (see Section 1, Introduction). On the basis of Eq. (1), the corresponding relaxation matrix of ^{17}O-water in such a system is a two-state hybrid which can be expressed as:

$$\boldsymbol{R}^{(n)}_{\text{system}} = p_{\text{sb}}\boldsymbol{R}^{(n)}_{\text{sb}} + p_{\text{'free'}}\boldsymbol{R}^{(n)}_{\text{'free'}} \tag{5}$$

or more conveniently as:

$$\boldsymbol{R}^{(n)}_{\text{system}} = p_{\text{sb}}\boldsymbol{R}^{(n)}_{\text{sb}} + (1 - p_{\text{sb}})\boldsymbol{R}^{(n)}_{\text{'free'}} \tag{6}$$

where the subscripts sb and 'free' refer to the strongly bound and free water, respectively. The quotes on the subscript 'free' are used to distinguish this term from the one which is used below. Although the two-state model was useful for characterising strongly bound water in different protein solutions, it was nevertheless 'incomplete', especially in accounting for the unusually large relaxation-rate constant obtained for 'free' water [6]. It was pointed out in that work that water molecules which are wea-kly bound to the macromolecule could possibly contribute significantly to the calculated relaxation rate constant of free water and therefore they should be included in a revised model of the system.

Weakly bound, or vicinal, water molecules have short correlation times that have been estimated to be less than 1 ns [18]. In NMR experiments performed on ^{17}O-water, at the Larmor frequency ($\frac{\omega_0}{2\pi}$) of 54 MHz, it is expected that the weakly bound water will not contribute significantly to the multiple-quantum filtered signal which is ultimately recorded, but it will considerably increase the relaxation rate of the free water. Hence, in the presence of weakly bound water, Eq. (6) may be viewed as a relaxation matrix expression for a pseudo two-state fast-exchange model in which the second term on the right hand side of this equation corresponds to the sum of the relaxation rate constants for the free and weakly bound water. Thus the equation can be rewritten as:

$$(1 - p_{\text{sb}})\boldsymbol{R}^{(n)}_{\text{'free'}} = p_{\text{wb}}\boldsymbol{R}^{(n)}_{\text{wb}} + (1 - p_{\text{sb}} - p_{\text{wb}})\boldsymbol{R}^{(n)}_{\text{free}} \tag{7}$$

where wb refers to weakly bound water. On the basis of Eqs. (6) and (7), it is easy to see that incorporation of a third state of water into the pseudo two-state model yields a modified equation:

$$\boldsymbol{R}^{(n)}_{\text{system}} = p_{\text{sb}}\boldsymbol{R}^{(n)}_{\text{sb}} + p_{\text{wb}}\boldsymbol{R}^{(n)}_{\text{wb}} + (1 - p_{\text{sb}} - p_{\text{wb}})\boldsymbol{R}^{(n)}_{\text{free}} \tag{8}$$

Eq. (8) describes the relaxation for a three-state fast-exchange model of water in the presence of biomolecules. The equation is similar to Eq. (4) introduced by Denisov and Halle in a recent ^{17}O-water relaxation-dispersion study [18]. It is important

to note that the three-state model could still be an over-simplification for large biomolecular systems which are expected to contain several different water-binding sites. Both the pseudo two-state and three-state fast-exchange models were used in our analysis of the TQF signals (Section 2.2).

2.2. Estimation of the fraction of strongly bound water

Chung and Wimperis [15] introduced a direct iterative fitting procedure to analyse spin-$\frac{5}{2}$ multiple-quantum relaxation in a two-state system undergoing fast chemical-exchange. In this method, the relaxation parameters such as τ_{sb} and the exchange-averaged quadrupolar constant, were directly determined by numerical comparison of the theoretical decay function with the observed signal decay. In the present work, a similar approach was implemented for analysing TQF data. However, as in our previous work [6], it was *assumed* that the 'quadrupolar constant' $\left(\frac{e^2qQ}{h}\right)\left(1+\frac{\eta^2}{3}\right)^{\frac{1}{2}}$ for strongly bound water is 7.6 MHz. This enabled the fraction of strongly bound water p_{sb} to be estimated.

2.2.1. Reduction of the number of parameters

In estimating the parameter values with the direct iterative method we found it useful to obtain initial estimates by using the two-state fast exchange model (Eq. (6)), because of its smaller number of parameters. The correlation time of the weakly bound water, τ_{wb}, was assumed to be considerably less than 1 ns so the system approximated well the extreme-narrowing limit ($\omega_0\tau_{wb} \ll 1$) and thus would not generate observable transverse TQF signals. As a consequence, the relaxation matrix $\boldsymbol{R}^{\mathbf{1}}_{\cdot free\cdot}$, which refers to the combined relaxation matrix of free and weakly bound water, is simpler since it will be 'almost diagonal' and thus similar to that of pure water in the extreme-narrowing limit. $\boldsymbol{R}^{\mathbf{1}}_{\cdot free\cdot}$ can then be characterised by a single relaxation rate constant, $R_{\cdot free\cdot}$ [15] which refers to either longitudinal or transverse relaxation. If only odd-rank coherences are considered, $\boldsymbol{R}^{\mathbf{1}}_{\cdot free\cdot}$ is equivalent to $\boldsymbol{R}^{\mathbf{0}}_{\cdot free\cdot}$ and can be written using the irreducible-operator basis as:

$$\boldsymbol{R}^{\mathbf{1}}_{\cdot free\cdot} = \begin{bmatrix} R_{\cdot free\cdot} & 0 & 0 \\ 0 & \frac{33}{8}R_{\cdot free\cdot} & 0 \\ 0 & 0 & \frac{15}{8}R_{\cdot free\cdot} \end{bmatrix} \qquad (9)$$

The elements of this matrix are defined according to Eqs. (5) and (6) shown in our previous work [6].

2.2.2. Unconstrained direct iterative method

The unconstrained iterative fitting procedure, for determining the parameter values for strongly bound water, using TQF data, operated as follows. First, a trial set of parameter values consisting of the correlation time of strongly bound water, τ_{sb}, the population fraction p_{sb}, and the apparent $R_{\cdot free\cdot}$ were used to construct a trial relaxation matrix for a pseudo two-state model. Second, this was then diagonalized to yield a TQF decay function $f_{31}^{(1)}(t)$ which was then multiplied by a trial scaling factor A and then numerically compared with the experimental decay data by obtaining the sum-of-squares of the residuals. Finally, the deviation from the experimental data was minimised by simultaneous optimisation of the four parameters (τ_{sb}, p_{sb}, $R_{\cdot free\cdot}$, and A) using a non-linear least-squares procedure.

Fig. 1 shows the results of the TQF experiments and the regression analysis for 30% (w/w) BSA. The experimental points are TQF signal intensities obtained with various values of the echo-time τ_e, as described in Section 3. These points were fitted with a TQF function, $Af_{31}^{(1)}(t)$. From Fig. 1, it is seen that there was good agreement between the experimental points and the fitted curve.

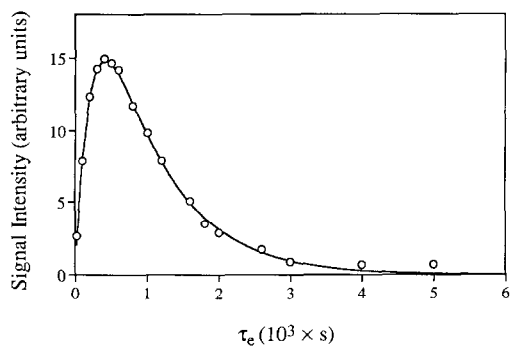

Fig. 1. Curve fitting of Eq. (6) using the ^{17}O-water transverse triple-quantum filtered signals (TQF) for 30% (w/w) BSA. The experimental TQF signal intensities (○) are plotted as a function of the experimental delay τ_e. The curve (——) was obtained by unrestricted direct iterative fitting yielding $\tau_{sb} = 9$ ns, $p_{sb} = 0.5\%$, $R_{\cdot free\cdot} = 600\,s^{-1}$ and $A = 163$. A similar curve was obtained with the parameter set $\tau_{sb} = 28$ ns, $p_{sb} = 0.2\%$, $R_{\cdot free\cdot} = 669\,s^{-1}$ and $A = 143$.

2.2.3. Limitation of the unconstrained iterative method

Although the analysis of ^{17}O-water TQF signals by regression analysis can yield estimates of the parameters relating to the bound water, the procedure has some shortcomings. These arise from the fact that there are several parameters which need to be optimised simultaneously, and the signal decay is not strictly described by a simple single exponential function. In other words, there were various combinations of τ_{sb}, p_{sb}, R_{1free}, and A which fitted the experimental data; this, of course, was especially true when signals were weak and the sums-of-squares of residuals were large. For example, in the curve fitting for 30% (w/w) BSA, shown in Fig. 1 the parameter set $\tau_{sb} = 9$ ns, $p_{sb} = 0.5\%$, $R_{1free} = 600\,s^{-1}$ and $A = 163$, fitted the experimental data as well as the parameter set $\tau_{sb} = 28$ ns, $p_{sb} = 0.2\%$, $R_{1free} = 669\,s^{-1}$ and $A = 143$. Different sets of values were usually obtained from different sets of initial parameters using a particular 'tolerance level' to define convergence of the minimization. Thus, it was difficult to decide rationally which of these parameter sets was the 'correct' one, especially if a range of likely parameter values was not available.

This dilemma can be readily seen from Fig. 2, which shows the dependence of the spin-echo TQF signal profile on (A) τ_{sb}, (B) p_{sb} and (C) R_{1free} in the range of values obtained in the curve fitting. The signals in each set were scaled so that their respective maximum value points were equal. One observes that the form of the signal profile, with the three parameters, were similar, particularly for the variation with τ_{sb} and p_{sb}. This similarity clearly showed that it was likely that there would be several combinations of τ_{sb}, p_{sb}, and R_{1free} which fitted a given set of data. It was therefore quite common to obtain parameter sets which were physically unrealistic.

2.2.4. Restricted direct iterative method

On the basis of the above findings, it appeared that the unconstrained direct iterative method was unreliable for the simultaneous determination of τ_{sb} and p_{sb} from the decay of the transverse TQF signal of ^{17}O-water. However, closer inspection of this method showed that a unique reproducible parameter-set could be obtained if the parameter value for

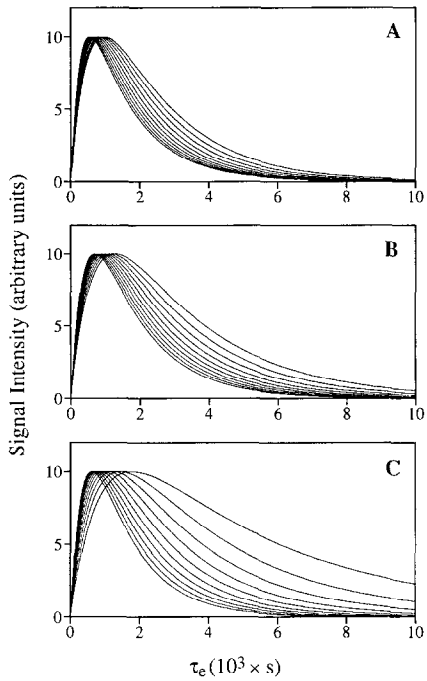

Fig. 2. Variation of the theoretical ^{17}O-water TQF signal profiles with (**A**) τ_{sb}, (**B**) p_{sb} and (**C**) R_{1free}. All signal profiles were scaled so that the maximum values for each set were equal. (**A**) $p_{sb} = 0.002$, $R_{1free} = 320\,s^{-1}$, and τ_{sb} values ranged from 3 to 30 ns in 10 equal increments; (**B**) $\tau_{sb} = 10$ ns, $R_{1free} = 320\,s^{-1}$, and p_{sb} values ranged from 0.0003 to 0.003 in 10 equal increments; (**C**) $\tau_{sb} = 10$ ns, $p_{sb} = 0.002$, and R_{1free} values ranged from $50\,s^{-1}$ to $500\,s^{-1}$ in 10 equal increments. In all cases the steepest curve corresponds the highest value of the varied parameter.

either τ_{sb} or p_{sb} were held constant during the fitting. Thus, in order for this procedure to be useful, the value of one of the parameters must be known, or at least constrained, in a domain of possible values. The actual values, or their possible ranges, were obtained from the results of other related studies.

Thus, we *fixed* the value of τ_{sb} and restricted the range of possible values for R_{1free} in order to gain information on the p_{sb} in different protein systems. The values of the correlation times τ_{sb} were based on the results of an NMR relaxation-dispersion study of various aqueous protein solutions by Halle et al. [4]. In this study the bound water had a correlation time, referring to slow motion, on a time scale ranging from 8–25 ns, depending on the particular protein.

The value of the longitudinal or transverse relaxation rate constant, $R_{1,\mathrm{free}}$, was constrained according to the longitudinal relaxation rate constant, $R_{\mathrm{system}}^{(0)}$ obtained from inversion recovery experiments on the various protein solutions. This restriction was based on the assumption that the longitudinal relaxation of ^{17}O-water in the protein systems is basically monoexponential [19,20]. The standard monoexponential longitudinal rate constant equation is:

$$R^{(0)} = \left(\tfrac{16}{5}\right) K\left[2J_1 + 8J_2\right] \qquad (10)$$

where K is a coefficient which contains the quadrupolar coupling constant [15], and J_1 and J_2 are the spectral density functions. On the basis of Eqs. (5) and (8), the longitudinal relaxation rate constant of the ^{17}O-water in protein solutions obeys the equation,

$$R_{\mathrm{system}}^{(0)} = p_{\mathrm{sb}}\left(\tfrac{16}{5}\right) K\left[2J_1^{\mathrm{sb}} + 8J_2^{\mathrm{sb}}\right] + \left(1 - p_{\mathrm{sb}}\right) R_{1,\mathrm{free}} \qquad (11)$$

where the first term on the right-hand side of the equation refers to the longitudinal relaxation rate-constant contribution from the strongly bound water. The importance of this equation is that the apparent relaxation rate constant, $R_{1,\mathrm{free}}$, is constrained so that its value cannot exceed $R_{\mathrm{system}}^{(0)}$ during the iterations.

2.3. Estimation of the fraction of weakly bound water

The fraction of weakly bound water, p_{wb}, was calculated by first assuming values for the correlation time and quadrupolar coupling constant. In the relaxation dispersion study of ^{17}O-water in different protein systems by Halle et al. [4] it was found that the correlation time relating to fast motion ranged from 9–25 ps and was basically independent of the type of protein. In the present study, we assumed that the weakly bound water had a correlation time of $\tau_{\mathrm{wb}} = 20$ ps and its quadrupolar coupling constant was equal to that of pure water. From the optimised parameters, p_{sb} and $R_{1,\mathrm{free}}$, which were obtained in the restricted iteration, we then indirectly estimated p_{wb} using a monoexponential longitudinal relaxation equation based on Eq. (6), viz.:

$$\left(1 - p_{\mathrm{sb}}\right) R_{1,\mathrm{free}} = p_{\mathrm{wb}}\left(\tfrac{16}{5}\right) K\left[2J_1^{\mathrm{wb}} + 8J_2^{\mathrm{wb}}\right] + \left(1 - p_{\mathrm{sb}} - p_{\mathrm{wb}}\right) R_{\mathrm{free}} \qquad (12)$$

The value for R_{free} was obtained from an inversion–recovery experiment on pure water.

3. Materials and methods

3.1. Materials

Solutions of BSA, BPTI, and lysozyme were prepared by dissolving measured masses of the proteins in pure D_2O of known mass. No further enrichment with $H_2{}^{17}O$ was used, but note that we found its concentration to be ~ 1.6 times as high as in normal distilled water (data not shown). BSA (fraction V) and lysozyme were obtained from Sigma (St. Louis, MO) while the BPTI was a gift from Bayer (Germany). The concentration of the protein in solution is reported as a percentage of the total weight of the sample, viz. w/w.

The solution of oxyhaemoglobin was prepared as described elsewhere [21]. A solution of 8% (w/w) haemoglobin (Sigma) was passed through an ion-retardation column (Biorad AG II, 1.5×25 cm) at a flow rate of 30 mL h^{-1}. After reconcentration using an Amicon PM 10 membrane, the solution was mixed with an equal volume of 10 mg mL^{-1} sodium dithionite and applied to a mixed-bed ion-exchange column (Biorad AG 501-X8, 1.4×50 cm) at a flow rate of 150 mL h^{-1}. The resulting solution of deoxyhaemoglobin was reconcentrated and washed several times by ultrafiltration in D_2O to yield a final concentration of $\sim 18\%$ (w/w). The sample was gently bubbled with O_2 for 20 min and then dispensed into a 'J. Young-Valve' NMR tube (Wilmad, NJ) and sealed under a pressure of ~ 150 kPa of oxygen.

3.2. NMR spectroscopy

All ^{17}O NMR experiments were performed on a Bruker AMX-400 wide-bore spectrometer operating at 54.24 MHz, and 298 K. Except for the BPTI samples in which a Wilmad 730 μL microcell was employed, conventional NMR tubes of 10-mm outer diameter were used and the sample volume was ~ 3 mL. The duration of a 90° r.f. pulse was ~ 21 μs. For most experiments, the acquired FID was digitised into 1 k complex points with a spectral width of 8 kHz; acquisition time was 64 ms; and the effective

relaxation recovery delay was ~ 65 ms. Data were processed by applying a 50 Hz line-broadening exponential factor prior to Fourier transformation.

For determination of the longitudinal relaxation time, inversion-recovery experiments were performed using a $90°_x-180°_y-90°_x$ composite inversion-pulse, and the data were analysed by a simultaneous 3-parameter fit to the predicted decay of $M[1 - C \exp(-R_{long} t)]$.

For TQF relaxation-rate analysis, a spin-echo pulse sequence was used which was identical to the multiple-quantum filter sequence of Ref. [15], which is $90°-\tau_e/2-180°-\tau_e/2-70.5°-\tau_m-90°-$acq(t), with appropriate phase cycles. To obtain the necessary relaxation–decay profiles, pseudo two-dimensional experiments were performed in which the echo-delay τ_e was varied. In all cases, the 'mixing' time τ_m was kept to a minimum value of 4 μs while acquisition was started after a delay of 88 μs from the last 90° pulse.

3.3. Error analysis

The estimates of the precision of parameter values, which were calculated from the results of non-linear least squares analyses of TQF signals and experimentally measured values, were obtained using the general procedure for 'propagation of errors' [22]. For this error analysis it was assumed that there was no statistical interaction between parameters so that covariance terms in the estimated errors could be neglected. The precision of the calculated values were reported as ± standard deviations.

4. Results and discussion

4.1. BSA solutions

In order to assess the utility of the TQF relaxation analysis, the experiments were first performed on BSA solutions of different concentrations; Fig. 3 shows the TQF signal intensity as a function of the echo-delay, τ_e, for the various solutions. The data were scaled so that the maximum values in each set were equal. It might be expected that the TQF signal would increase with increasing protein concentration, and while this trend was evident in the range up to ~ 20% (*w*/*w*), for greater concentrations the maximum amplitudes were smaller as a result of increased line-broadening.

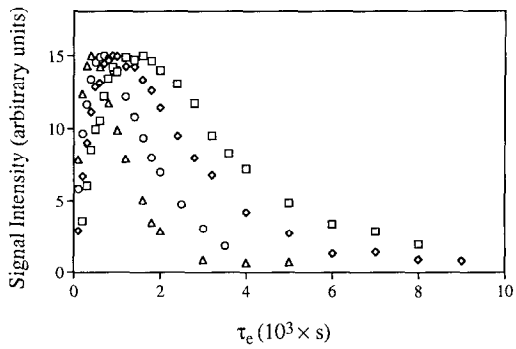

Fig. 3. ^{17}O-water TQF signal intensities for the 8% (□), 13% (◇), 20% (○) and 30% (△) (*w*/*w*) BSA solutions, plotted as a function of the pulse-sequence delay τ_e. The maximum value in each set was scaled so that it was equal in each case.

Fig. 3 shows that as the concentration of BSA was increased the TQF-signal curves became steeper, and the maximum amplitude shifted to a lower τ_e value. These effects indicated that the TQF signal relaxation rates were faster in the more concentrated solutions, which is consistent with the correlation time of the protein being higher (see Discussion).

The TQF transverse-relaxation data on bound water in BSA solutions are summarised in Table 1. The parameter values were obtained assuming correlation times for strongly and weakly bound water of τ_{sb} = 15 ns and τ_{wb} = 20 ps, respectively. These values were based on a NMR relaxation–dispersion study of ^{17}O-water in solutions of human plasma albumin [4] in which the correlation times were found to be 16 ns and 17 ps, respectively; but because the former values did not refer directly to BSA we rounded the values to a nearby multiple of five. R_{long} values presented in Table 1 were obtained from inversion–recovery experiments and were used as constraints in the relaxation analysis.

From Table 1 it is clear that the calculated fraction of bound water p_{sb} increased with an increase in BSA concentration. Values for p_{sb} ranged from 0.02 × 10^{-3} for 5% (*w*/*w*) BSA to 4.20 × 10^{-3} for 30% (*w*/*w*) BSA. The p_{sb} value for 5% (*w*/*w*) BSA was low, which suggests that the *actual* τ_{sb} for BSA at this concentration would be much smaller than the assumed value of 15 ns. (The use of the literature

Table 1
^{17}O-water relaxation data for BSA solutions[a]

Amount BSA (%w/w)	R_{long} (s^{-1})	$(1-p_{sb})R_{1free}$ (s^{-1})	p_{sb} ($10^3\times$)	p_{wb}	$n_{sb}/_{BSA}$	$n_{wb}/_{BSA}$
0	189.1 ± 0.4	0	0	0	–	–
5	233.7 ± 0.4	233.4 ± 0.4	0.02 ± 0.01	0.049 ± 0.001	1 ± 1	3040 ± 40
8	264.2 ± 0.8	259.0 ± 1.1	0.42 ± 0.06	0.077 ± 0.001	16 ± 2	2960 ± 50
10	286.5 ± 1.1	280.7 ± 1.2	0.47 ± 0.04	0.101 ± 0.001	14 ± 1	3000 ± 40
13	327.7 ± 1.2	316.9 ± 1.3	0.88 ± 0.04	0.141 ± 0.001	20 ± 1	3180 ± 30
16	354.8 ± 1.6	339.2 ± 1.8	1.27 ± 0.06	0.166 ± 0.002	22 ± 1	2880 ± 30
20	425.0 ± 4.7	399.7 ± 4.9	2.14 ± 0.11	0.233 ± 0.005	28 ± 1	3060 ± 70
30	562.2 ± 5.4	510.6 ± 5.7	4.20 ± 0.16	0.356 ± 0.006	32 ± 1	2720 ± 50

[a]The following correlation times were assumed; τ_{sb} = 15 ns and τ_{wb} = 20 ps. n_{sb} = number of strongly bound water molecules. n_{wb} = number of weakly bound water molecules.

value of 16 ns for τ_{sb} [4] instead of 15 ns led to less than a 10% decrease in the estimate of p_{sb}.) Thus the p_{sb} values at this point must be considered to be only *apparent* ones.

To investigate this point further, Fig. 4 shows graphs of p_{sb} for the BSA samples assuming correlation times (τ_{sb}) ranging from 5 to 30 ns. It is clear that the increase in p_{sb} with concentration was greater than linear for all cases, indicating that in the experiments there was probably an increase in the correlation time with increasing BSA concentration. This effect was seen in the plot for which τ_{sb} = 5 ns, so this indicates that it is incorrect to assume only one value of τ_{sb} for BSA. Specifically, it is known that the overall correlation time τ_r of a protein will

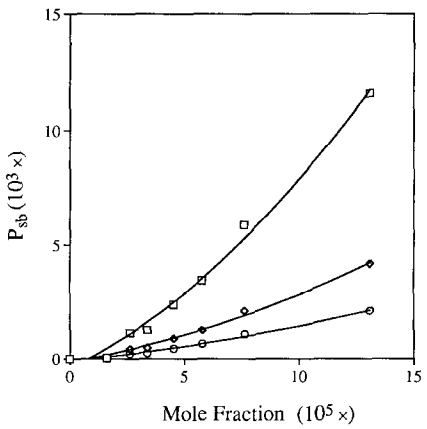

Fig. 4. Calculated p_{sb} values for water, as a function of mole fraction of BSA in the solution. The results are shown for assumed τ_{sb} values of 5 ns (□), 15 ns (◇), and 30 ns (○). The fitted curves are empirical second-order polynomials.

increase with increasing concentration [18] and that τ_{sb} will become equal to τ_r when the residence time of the strongly bound water is long.

A ^{17}O-water study of the effect of increasing protein concentration [4] has confirmed that the correlation times for slow-motion of the bound water (which corresponds to τ_{sb} in this study) increases with increasing protein concentration. This effect, which is attributed to enhanced electrostatic repulsion between protein molecules, was seen in a graph of relaxation rate-constant versus protein concentration. Similarly, Fig. 5 shows the plot of observed ^{17}O-water longitudinal relaxation rate-constant, R_{long}, with protein concentration expressed in % *w/w* (A) and mol% (A). The relaxation plot is *non*-linear for Fig. 5A but linear for Fig. 5B. The non-linearity of the data in Fig. 5A is similar to that obtained in the above mentioned study [4] where it was attributed to an increase in correlation time of the slow motion of bound water, with increasing protein concentration. This conclusion is questionable since Fig. 5A was based on a plot in which the concentration of the protein (expressed in weight percent) does not reflect the real protein:water molar ratio in the solution. The plot in Fig. 5B is more consistent with the physical interpretation of the binding system, and the linearity of the plot suggests that there was no significant change in the correlation time of the tightly bound water, contrary to the conclusion reached on the basis of the data in Fig. 4.

The results given in Table 1 also show that there was an increase in $(1-p_{sb})R_{1free}$ (that is approximately equal to R_{1free}) with increasing BSA concen-

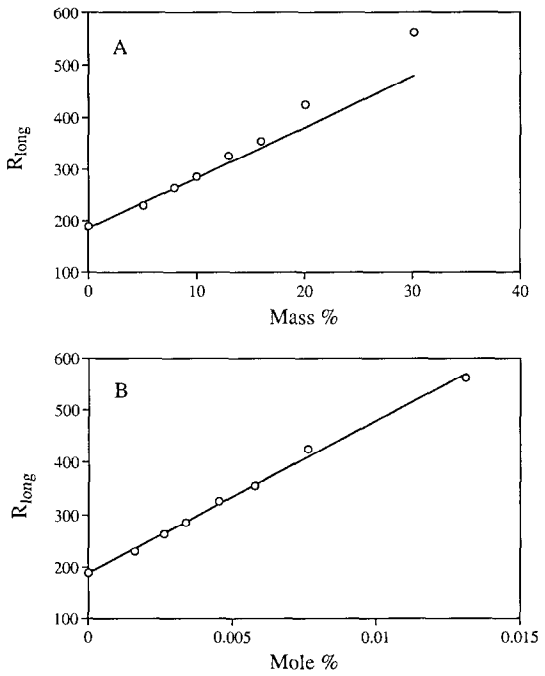

Fig. 5. Plots of the ^{17}O-water longitudinal relaxation rate constants (○) in BSA solution as a function of protein concentration expressed as: (**A**) mass ratio, % *w/w*, and (**B**) mol%. The straight line in (**A**) was drawn to emphasise the non-linearity of the data.

tration; this is in good agreement with the results of our previous study [6]. This trend clearly demonstrates the increased relaxation contribution from weakly bound water, the magnitude of which was quite pronounced considering that the measured R_{long} of pure water (R_{free}) was only 189.1 s^{-1}. The values of p_{wb} estimated from R_{1free}, increased with increasing BSA concentration, in a manner similar to the observed trend in p_{sb} values. Thus these values, which ranged from 0.049 (5% *w/w* BSA) to 0.356 (30% *w/w* BSA), were approximately a hundred times greater than the p_{sb} values.

The calculated p_{sb} and p_{wb} values were used to estimate the number of water molecules associated with each BSA molecule. Except for 5% (*w/w*) BSA, the apparent number (shown in Table 1) ranged from 14 to 32 while that for the weakly bound water range from 2720 to 3180. The apparent number of *strongly* bound water molecules increased with increasing BSA concentration. However, as stated above, this interpretation is flawed since the number of water binding sites should be concentration-independent in the absence of processes such as protein polymerisation. Thus, the trend in apparent value of p_{sb} is most probably due to an increase in the correlation times, τ_r or τ_{sb}, with protein concentration. In contrast, there appears to be no definite trend in the number of apparently *weakly* bound water molecules per BSA molecule, which is a result consistent with the actual value of τ_{wb} remaining unchanged.

4.2. Other protein solutions

TQF transverse-relaxation analysis was applied to solutions of three other proteins in order to characterise and compare the properties of the bound water present in each. The solutions studied were approximately 18% (*w/w*) of lysozyme, oxyhaemoglobin (oxyHb), and BPTI. To facilitate comparison of results, analyses were performed assuming two τ_{sb} values; one at 15 ns and the other being the slow-motion correlation times (τ_{slow}) obtained from ^{17}O-water NMR relaxation dispersion analysis [4,18]. In the latter studies, the calculated correlation times for BPTI, lysozyme, and oxyHb and were 7 ns, 19 ns, and 25 ns, respectively. On the other hand, it was assumed that the correlation time of weakly bound water, τ_{wb}, was 20 ps in all the protein solutions.

Fig. 6 shows the spin-echo TQF signal-intensity for different protein solutions as a function of the delay, τ_e. The data were plotted so that the maximum

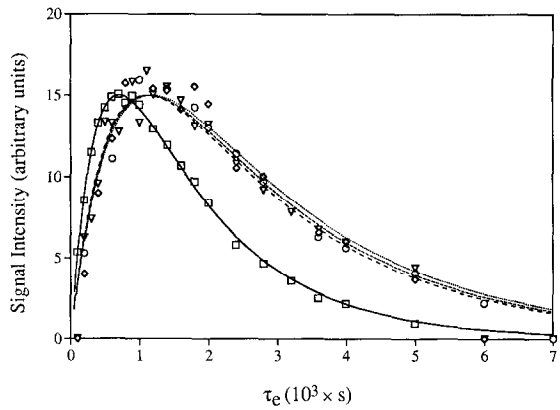

Fig. 6. Comparison of the ^{17}O-water TQF signals obtained in 18% (*w/w*) solutions of BSA (□, ——), BPTI (◇, · · ·), lysozyme (○, - - -), and oxyhaemoglobin (▽, – – –). The experimental data points were scaled so that the maximum fitted values in each set were equal.

value of the best-fit curve was the same in all cases. Fig. 6 shows that the data from BPTI, lysozyme, and oxyhaemoglobin were less precise than those from BSA. This was mainly due to the lower signal-to-noise in the spectra obtained for these three proteins. Also the BSA data lay on a steeper curve (Section 4.1), compared with oxyhaemoglobin, BPTI and lysozyme, all of which showed similar profiles.

In order to convey an impression of the sensitivity of the analysis to changes in τ_{sb} and p_{sb} we, first, supposed that the values of τ_{sb} of these proteins were all the same value of 15 ns. Thus, according to the results given in Table 2 it would be concluded that BSA has considerably more strongly bound water molecules than the other three proteins. On the other hand when the previously mentioned τ_{sb} values were used there were also wide variations in the calculated p_{sb} value for each protein solution; however, the BSA solution still had the highest fraction of strongly bound water, 1.80×10^{-3}. This was anticipated from its 'steep' TQF signal profile and high signal-to-noise ratio in the spectra. Although the TQF signal profiles for BPTI, haemoglobin and lysozyme were similar, the calculated p_{sb} values were very dependent on the assumed τ_{sb} values, as shown by the magnitude of the changes in p_{sb} for BPTI, Lysozyme and Hb when τ_{sb} was varied away from 15 ns. The largest difference was obtained for BPTI in which p_{sb} increased from 0.60×10^{-3} to 1.21×10^{-3} when the assumed value of τ_{sb} was changed from 15 ns to 7 ns. Thus, this confirmed findings presented earlier that it is important to have a good estimate of the correlation time of the strongly bound water, or the protein.

Other data obtained from the TQF relaxation analysis are also summarised in Table 2: the longitudinal relaxation rate constant, R_{long}, varied considerably between protein solutions, with BSA showing the highest value of $388\,s^{-1}$, and BPTI showing the lowest value, $295\,s^{-1}$. For BPTI, the smaller longitudinal relaxation rate constant compared with Hb, and lysozyme, suggests that $R_{1,free}$ was also smaller, so p_{sb} was adjusted to a higher value during the iteration.

In summary, although the TQF signal-profiles for the three protein solutions were comparable, the lower longitudinal relaxation rate constant for BPTI implied that its fraction of strongly bound water was higher. The same rationale explains why p_{sb} values estimated for haemoglobin and lysozyme were similar. With regard to the number of strongly bound water molecules per protein molecule, when τ_{sb} = 15 ns, BSA had the largest number, while BPTI and lysozyme had the least. Although the molecular mass of BSA (66 000 Da) and oxyhaemoglobin (64 500 Da) are similar, the number of strongly bound water molecules in BSA (27) was about four times greater. BPTI and lysozyme had almost the same number of strongly bound water molecules, estimated to be ~ 1; although the molecular mass of lysozyme (14 400 Da) is about twice that of BPTI (6500 Da). Hence, for the four proteins considered in this study, there appears to be no simple correlation between the number of strongly bound water molecules and the mass of the protein. In contrast to this trend for the strongly bound water, the number of weakly bound water molecules was proportional to the molecular mass of the protein.

Table 2
^{17}O-water relaxation data for 18% (w/w) solutions of different proteins[a]

Protein system[b]	R_{long} (s^{-1})	p_{sb} ($10^3 \times$)	p_{wb}	$n_{sb}/_{pro}$	$n_{wb}/_{pro}$
a) τ_{sb} = 15 ns					
BSA	388 ± 2	1.80 ± 0.05	0.196 ± 0.002	26.6 ± 0.7	2900 ± 30
BPTI	295 ± 4	0.60 ± 0.15	0.109 ± 0.005	0.9 ± 0.2	160 ± 7
Lys	334 ± 1	0.42 ± 0.10	0.154 ± 0.002	1.4 ± 0.2	504 ± 6
oxyHb	348 ± 1	0.40 ± 0.10	0.170 ± 0.002	6 ± 2	2600 ± 30
b) τ_{sb} variable					
BPTI (τ_{sb} = 7 ns)	295 ± 4	1.21 ± 0.30	0.085 ± 0.009	1.8 ± 0.4	120 ± 13
Lys (τ_{sb} = 19 ns)	334 ± 1	0.34 ± 0.08	0.156 ± 0.001	1.1 ± 0.3	511 ± 5
oxyHb (τ_{sb} = 25 ns)	348 ± 1	0.24 ± 0.06	0.174 ± 0.001	3.7 ± 0.9	2700 ± 20

[a] In all cases τ_{wb} was assumed to be 20 ps.
[b] Lys = lysozyme, oxyHb = oxyhaemoglobin.

In the analysis of the weakly bound water fraction p_{wb}, it was found that values for BSA, Hb, and lysozyme were similar and occurred over a narrow range between 0.150 to 0.200. The estimates of p_{wb} for BPTI was found to be much smaller than for BSA at ~0.100. Variation of the assumed τ_{sb} values in the analysis did not significantly alter the estimate of p_{wb}.

It is important to compare the results of this TQF relaxation study to those of other studies of protein hydration employing similar proteins. Otting et al. [2] showed that there are four internal water molecules in BPTI which are bound sufficiently tightly to give signals in a two-dimensional nuclear Overhauser enhancement spectroscopy (NOESY) experiment. On the other hand, a recent relaxation–dispersion study [18], showed that there are only two observable strongly bound water molecules in BPTI (which have an effective correlation time of 7 ns). It is believed that the remaining two water molecules were not observed because one is deeply buried in a 'cavity' in the BPTI molecule and therefore does not exchange with the free water while the other is held more loosely in the hydrogen-bonding network so that it is more 'disordered' than the two strongly bound water molecules. From Table 2 it is noted that if a 7 ns correlation time is assumed then the fraction of strongly bound water is calculated to be 1.8 and this agrees with the number obtained using the NMR relaxation–dispersion method [18].

Colombo et al. [23] studied the hydration of oxyhaemoglobin by 'osmotic stress' and showed that ~60 water molecules are associated with it during transition from deoxyhaemoglobin to oxyhaemoglobin. It is not possible to perform a reliable TQF experiment on deoxyhaemoglobin because the signals are broadened considerably because of its paramagnetism. Table 2 (with $\tau_{sb} = 25$ ns) indicates that there are four strongly bound water molecules and 2700 weakly bound ones associated with each oxyhaemoglobin molecule. These findings are difficult to reconcile with those obtained by the osmotic stress method, since the nature of the binding of the putative '60' water molecules is not known. However, it is possible that some of the water molecules observed in the osmotic stress study are strongly bound but are not chemically exchanging sufficiently rapidly with the bulk water so that, in turn, they are not observed in the TQF experiment.

4.3. Longitudinal relaxation rate contributions from different states of water

It is instructive to determine the relative contribution of the different states of water to the *total* longitudinal relaxation rate constant for the various proteins employed in this work. These values were determined by using Eqs. (8) and (10), and the fractions of bound water obtained earlier.

Table 3 shows relative relaxation rate constant contributions from the three states of water for the various 18% (w/w) protein solutions, at 298 K. For

Table 3
^{17}O-longitudinal relaxation rate constant contributions from the different states of water in different 18% (w/w) protein solutions[a]

Protein system[b]	Water state		
	Free (%)	Strongly bound (%)	Weakly bound (%)
a) $\tau_{sb} = 15$ ns			
BSA	39.1 ± 0.2	5.7 ± 0.2	55.2 ± 0.7
BPTI	57.1 ± 0.8	2.5 ± 0.6	40.4 ± 1.9
Lys	47.8 ± 0.2	1.5 ± 0.4	50.6 ± 0.6
oxyHb	45.0 ± 0.2	1.4 ± 0.4	53.5 ± 0.6
b) τ_{sb} variable			
BPTI ($\tau_{sb} = 7$ ns)	58.6 ± 1.0	10.0 ± 2.5	31.4 + 3.4
Lys ($\tau_{sb} = 19$ ns)	47.7 ± 0.2	1.0 ± 0.2	51.3 ± 0.5
oxyHb ($\tau_{sb} = 25$ ns)	44.9 ± 0.2	0.5 ± 0.1	54.6 ± 0.4

[a] In all cases, τ_{wb} was assumed to be 20 ps.
[b] Lys = lysozyme, oxyHb = oxyhaemoglobin.

each protein, significant proportions of the total longitudinal relaxation rate constant were due to free and weakly bound water. Relaxation rate contributions from strongly bound water were found to be smaller, generally less than 10%. With the assumption that $\tau_{sb} = 15$ ns, BSA showed the largest longitudinal relaxation rate constant, with contributions for both strongly (5.7%) and weakly bound water (55.2%).

4.4. Conclusions

Water molecules bound to proteins can be classified and quantified through the use of TQF relaxation analysis of ^{17}O-water. This procedure is very effective in discriminating between different water states since the TQF signal is produced only by the presence of exchanging strongly bound ^{17}O-water, with correlation times greater than 1 ns, and not by weakly bound or free ^{17}O-water in the solution. In comparison with our earlier study, which assumed a two-state fast-exchange model [6], the analysis described here assumed a three-state fast-exchange model so that population sizes of weakly bound, strongly bound, and free water could be determined. Quantification of the amount of bound water, however, required knowledge, or an estimate, of the correlation time of water tightly bound in the protein. The TQF NMR relaxation analysis of ^{17}O-water provides further insight into the various states of water in concentrated protein solutions and, by inference, inside cells. Thus, it contributes to the understanding of the altered hydrogen-bonding potential of water inside cells alluded to in Section 1.

Acknowledgements

The is work was funded by a project grant from the Australian NH & MRC. Dr. Evelyne Baguet is thanked for her contributions during the early experiments, Mr. Brian Bulliman for assistance with computing, Dr. Bill Bubb for assistance with the NMR spectrometer, and Bayer Australia Limited for providing the BPTI sample.

References

[1] R. Cooke, I.D. Kuntz, Ann. Rev. Biophys. Bioeng. 3 (1974) 95.
[2] G. Otting, E. Liepinsh, K. Wüthrich, Science 254 (1991) 974.
[3] P.S. Belton, Prog. Biophys. Mol. Biol 61 (1994) 61.
[4] B. Halle, T. Andersson, S. Forsén, B. Lindman, J. Am. Chem. Soc. 103 (1981) 500.
[5] C.W. Flesche, M.L.H. Gruwel, A. Deussen, J. Schrader, Biochim. Biophys. Acta 1244 (1995) 253.
[6] E. Baguet, B.E. Chapman, A.M. Torres, P.W. Kuchel, J. Magn. Reson. Ser. B 111 (1996) 1.
[7] K. Kirk, P.W. Kuchel, Biochemistry 27 (1988) 8795.
[8] K. Kirk, P.W. Kuchel, Biochemistry 27 (1988) 8803.
[9] J.A. Barry, K.A. McGovern, Y.H. Lien, B. Ashmore, R.J. Gillies, Biochemistry 32 (1993) 4665.
[10] J.R. Potts, P.W. Kuchel, Biochem. J. 281 (1992) 753.
[11] P.W. Kuchel, B.E. Chapman, A.S.-L. Xu, in: E. Bamberg, H. Passow (Eds.), Rates of Anion Transfer Across Erythrocyte Membranes Measured with NMR Spectroscopy (The Band 3 Proteins: Anion Transporters, Binding Proteins and Senescent Antigens), Elsevier, Amsterdam, 1992, p. 105.
[12] P.W. Kuchel, K. Kirk, G.F. King, in: H.J. Hilderson, G.B. Ralston (Eds.), NMR Methods for Measuring Membrane Transport (Physicochemical Methods in the Study of Biomembranes, Vol. 23), Plenum Press, New York, 1994, p. 247.
[13] H.A. Berthon, P.W. Kuchel, in: K.M. Brindle (Ed.), NMR Studies of Erythrocyte Metabolism (Advances in Molecular and Erythrocyte Cell Biology, Vol. 11), JAI Press Inc., 1995, p. 147.
[14] G. Jaccard, S. Wimperis, G. Bodenhausen, J. Chem. Phys. 85 (1986) 6282.
[15] C.-W. Chung, S. Wimperis, Mol. Phys. 76 (1992) 47.
[16] N. Müller, G. Bodenhausen, R.R. Ernst, J. Magn. Reson. 75 (1987) 297.
[17] T.E. Bull, J. Magn. Reson. 8 (1972) 344.
[18] V.P. Denisov, B. Halle, J. Mol. Biol. 245 (1995) 682.
[19] B. Halle, H. Wennerström, J. Magn. Reson. 44 (1981) 89.
[20] T.E. Bull, S. Forsén, D.L. Turner, J. Chem. Phys. 70 (1979) 3106.
[21] C. Bauer, B. Pacyna, Anal. Biochem. 65 (1975) 445.
[22] M. Kendall, A. Stuart, The Advanced Theory of Statistics, Griffin, London, 1977.
[23] M.F. Colombo, D.C. Rau, V.A. Parsegian, Science 256 (1992) 655.